

*This copy is for your personal, non-commercial use only.*

**If you wish to distribute this article to others**, you can order high-quality copies for your colleagues, clients, or customers by [clicking here](#).

**Permission to republish or repurpose articles or portions of articles** can be obtained by following the guidelines [here](#).

***The following resources related to this article are available online at [www.sciencemag.org](http://www.sciencemag.org) (this information is current as of May 3, 2010):***

**Updated information and services**, including high-resolution figures, can be found in the online version of this article at:

<http://www.sciencemag.org/cgi/content/full/328/5978/600>

**Supporting Online Material** can be found at:

<http://www.sciencemag.org/cgi/content/full/science.1184246/DC1>

This article has been **cited by** 1 articles hosted by HighWire Press; see:

<http://www.sciencemag.org/cgi/content/full/328/5978/600#otherarticles>

This article appears in the following **subject collections**:

Astronomy

<http://www.sciencemag.org/cgi/collection/astronomy>

# Major Galaxy Mergers and the Growth of Supermassive Black Holes in Quasars

Ezequiel Treister,<sup>1\*</sup> Priyamvada Natarajan,<sup>2,3,4\*</sup> David B. Sanders,<sup>1</sup> C. Megan Urry,<sup>2,3,4</sup> Kevin Schawinski,<sup>3,4</sup> Jeyhan Kartaltepe<sup>1,5</sup>

Despite observed strong correlations between central supermassive black holes (SMBHs) and star formation in galactic nuclei, uncertainties exist in our understanding of their coupling. We present observations of the ratio of heavily obscured to unobscured quasars as a function of cosmic epoch up to  $z \cong 3$  and show that a simple physical model describing mergers of massive, gas-rich galaxies matches these observations. In the context of this model, every obscured and unobscured quasar represents two distinct phases that result from a massive galaxy merger event. Much of the mass growth of the SMBH occurs during the heavily obscured phase. These observations provide additional evidence for a causal link between gas-rich galaxy mergers, accretion onto the nuclear SMBH, and coeval star formation.

While unobscured quasars (1) have been known for a long time (2) and their statistical properties are well studied (3), the numbers of the heavily obscured quasar population and its variation with cosmic epoch are still strongly debated. This population has been uncovered with multiwavelength selection techniques that simultaneously exploit x-ray (4), optical (5), and mid-infrared (mid-IR) (6) wavelengths. As a result of the efficiency of these techniques, the sample sizes of obscured quasars are growing substantially. The existence of a large number of heavily obscured quasars at  $z \sim 2$  was predicted by early active galactic nuclei (AGN) population synthesis models that successfully explain the generation of the x-ray background (7). However, their space density cannot be constrained by these calculations (8). What population these obscured sources evolve into or proceed from is poorly understood at present.

The link between ultraluminous infrared galaxies (ULIRGs) and quasars was first suggested by Sanders *et al.* (9). There is substantial observational evidence that ULIRGs, at least locally, are the product of the gas-rich merger of two massive [ $M \gtrsim 10^{11} M_{\odot}$  (solar mass)] galaxies (10). The merger process is believed to switch on accretion onto the central black hole as it provides efficient transport of gas to the nucleus (11). The gas funneled to the center is expected to fuel the supermassive black hole and induce star formation. The origin of the infrared luminosity of these sources, whether they are powered primarily by star-formation processes

(12) or the AGN (9) activity, is still debated. Here, we present recent measurements of the space density of heavily obscured quasars as a function of redshift and estimate the duration of the obscured stage by comparing models with observations.

Mainly due to the effects of dust and gas obscuration at most wavelengths, finding heavily obscured quasars (13) is a challenging task that has prevented the identification of larger samples, in particular, at high redshifts. Measuring their space density is even more difficult, as it requires a good knowledge of the selection function and observational biases. We have compiled observations of obscured quasars selected at various wavelengths using different techniques, described in detail in the supporting online material (SOM), including spectral fitting in x-rays (14) and IR selection (15–17). X-rays, especially at rest-frame energies greater than 10 keV, are not appreciably affected by obscuration. In addition, most of the absorbed energy is later reemitted at IR wavelengths. Thus, these techniques permit an estimate of the number of heavily obscured quasars at  $z > 1$ . In the local universe, the space density of ULIRGs (18), which can be used as an indicator of the total number of quasars, implies that the ratio of heavily obscured to unobscured quasars at  $z = 0.1$  is  $\sim 1$  (Fig. 1).

Both in the local universe and at  $z \cong 1$ , heavily obscured AGN are bright at mid- and far-IR wavelengths and also potentially in the submillimeter-wavelength range but are optically faint (Fig. 2). At low redshift, the ULIRG is clearly the product of a galaxy merger, whereas at high redshift a merger is suggested, but deeper data are needed to confirm this hypothesis. The rest-frame optical images of six heavily obscured quasar candidates show indications of ongoing major mergers and interactions (Fig. 3).

To interpret these observations and the evolution of these populations, we started with the standard ansatz that the gas-rich major merger of two massive galaxies produces one newly fueled quasar. This triggered quasar is originally obscured by the surrounding gas and dust (9), in some cases

reaching Compton-thick levels (i.e., where the optical depth for Compton scattering is greater than one). After a time  $\Delta t \sim 10^7$  to  $10^8$  years (19), which we estimate independently below, most of the dust and gas are removed from the central region and the quasar becomes unobscured.

To test this simple prescription, the calculated ratio of heavily obscured to unobscured sources from merger rates of massive gas-rich galaxies needs to match the observed ratio of obscured to unobscured quasars. This ratio can be calculated using the merger rate as a function of cosmic time in the context of the hierarchical cold dark matter (LCDM) structure formation paradigm. Using the assumptions described above, we estimated the ratio of obscured to unobscured sources as

$$\frac{N_{\text{obs}}}{N_{\text{unobs}}}(z) = \frac{\Delta t \frac{d^2 \text{Merger}}{dNdt} N_{\text{gal}}(> M_{\text{star}}(z)) f_g(z)}{N_{\text{unobs}}(z)} \quad (1)$$

where  $N_{\text{obs}}$  is the space density of heavily obscured quasars;  $d^2 \text{Merger}/dNdt$  is the merger frequency per galaxy per unit time;  $N_{\text{gal}}$  and  $N_{\text{unobs}}$  are the space densities of massive galaxies and unobscured quasars, respectively; and  $f_g$  is

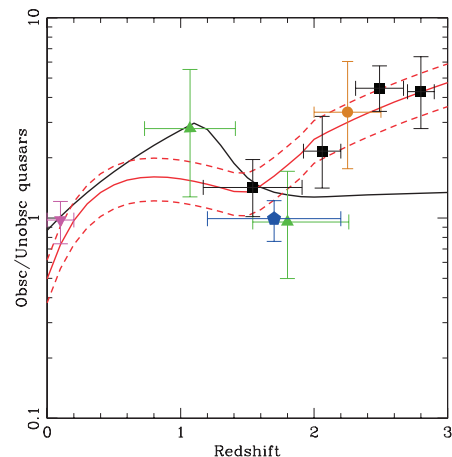


**Fig. 1.** The ratio of heavily obscured to unobscured quasars as a function of redshift. Measurements of the space density of obscured quasars at high redshift were obtained from x-ray [green triangles (14)] and mid-IR imaging [blue pentagon (16) and black squares (17)] and spectroscopy [brown circle (15)] selection techniques. For the  $z \cong 0$  measurement, we used the luminosity function of local ULIRGs (18), assuming that each ULIRG is either a heavily obscured or an unobscured quasar. The solid black line shows the heavily obscured to unobscured quasar ratio expected from AGN luminosity functions derived from hard x-ray observations (32), and the solid red line corresponds to the ratio obtained if every gas-rich major merger of two massive galaxies generates a heavily obscured quasar, which after a time  $\Delta t \cong 96$  My becomes unobscured. Dashed lines show the uncertainty in this relation, at the 90% confidence level.

<sup>1</sup>Institute for Astronomy, 2680 Woodlawn Drive, University of Hawaii, Honolulu, HI 96822, USA. <sup>2</sup>Department of Astronomy, Yale University, Post Office Box 208101, New Haven, CT 06520, USA. <sup>3</sup>Department of Physics, Yale University, Post Office Box 208121, New Haven, CT 06520, USA. <sup>4</sup>Yale Center for Astronomy and Astrophysics, Post Office Box 208121, New Haven, CT 06520, USA. <sup>5</sup>National Optical Astronomy Observatory, 950 North Cherry Avenue, Tucson, AZ 85719, USA.

\*To whom correspondence should be addressed. E-mail: treister@ifa.hawaii.edu (E.T.); priyamvada.natarajan@yale.edu (P.N.)

the average fraction of gas-rich galaxies. The major merger frequency per galaxy in the LCDM paradigm can be parameterized as a power-law in  $(1+z)$  with a mass-dependent exponent of  $\approx 1.5$  (20). This form is derived from model parameters constrained by observations. To estimate the space density of galaxies above a threshold stellar mass, we used the median mass measured for ULIRGs found in the Cosmic Evolution Survey (COSMOS). The median mass

increases with decreasing redshift, going from  $\sim 10^{11} M_{\odot}$  at  $z \sim 2$  to  $10^{11.3} M_{\odot}$  at  $z = 0.8$  (fig. S1). We then incorporated this limiting mass into the stellar mass function computed by Marchesini *et al.* (21) to obtain the space density of massive galaxies as a function of redshift. Rather than directly estimate the gas content of high-redshift galaxies, which is currently observationally impossible at these redshifts, we used the average star-formation rate as a proxy for

the evolution of the fraction  $f_g$  of gas-rich galaxies. The evolution of the star-formation rate can be approximated as  $(1+z)^2$  up to  $z \approx 2$ , remaining mostly flat at higher redshifts, on the basis of ultraviolet observations of galaxies up to  $z \approx 2.5$  (22). Finally, the space density of unobscured quasars,  $N_{\text{unobsc}}(z)$ , has been measured by both x-ray (23, 24) and optical (25) surveys, and consistent results are found with these two methods. These are all the ingredients needed to compute the expected fraction of obscured to unobscured quasars, wherein  $\Delta t$  in Eq. (1) can be determined as a free parameter. The redshift dependence of each of these components is shown in fig. S2.

The estimates from our simple scenario are consistent with the observations (Fig. 1), in particular considering the steep evolution in the relative number of obscured sources from  $z = 1.5$  to 3. This rapid increase is not predicted or expected from existing AGN luminosity functions (Fig. 1). That is, extrapolations from the behavior of less-obscured lower-luminosity sources (with observed column densities  $< 10^{23} \text{ cm}^{-2}$ ) do not match current observations, in particular at  $z > 2$ . This suggests the existence of a different channel for the triggering mechanism for quasars, compared to lower-luminosity AGN. The best-fit value of  $\Delta t$  we obtained is  $96 \pm 23$  million years (My; 90% confidence level). This is very similar to the current best estimates of quasar lifetimes in their optically bright, unobscured phases [10 to 100 My (26)], indicating that these sources spend roughly half their life in the obscured phase.

Having determined that quasars that are fueled by the merger of massive gas-rich galaxies spend comparable amounts of time in the obscured and unobscured phases, we then estimated the implications for the mass accretion onto the nuclear supermassive black holes during these two stages. Assuming a typical accretion efficiency of  $\epsilon = 0.1$ , the mass growth of the supermassive black hole due to accretion is given by

$$\Delta M_{\text{BH}} = 1.6 \times 10^7 \left( \frac{L_{\text{bol}}}{10^{45} \text{ erg/s}} \right) \left( \frac{T}{10^8 \text{ years}} \right) M_{\odot} \quad (2)$$

where  $T$  is the duration of the entire accretion episode that includes the obscured and unobscured phases. The typical bolometric luminosities of these sources span the range  $10^{45}$  to  $10^{47} \text{ erg/s}$  [ $\sim 10^{12}$  to  $10^{14} L_{\odot}$  (solar luminosity)], while they have black hole masses of  $M_{\text{BH}} \sim 10^8$  to  $10^{10} M_{\odot}$  (27, 28). Given that the typical duration of the total (both obscured and unobscured) luminous quasar phase is  $T \sim 2 \times 10^8$  years, it is possible for a quasar to build most or all of the black hole mass in a single event, which is triggered by a major merger as suggested here.

In spite of copious accretion, due to their high redshifts and strong absorption, this unexpected population of obscured quasars are not key contributors to the extragalactic x-ray background radiation. Their total contribution is estimated to be  $\sim 1$  to

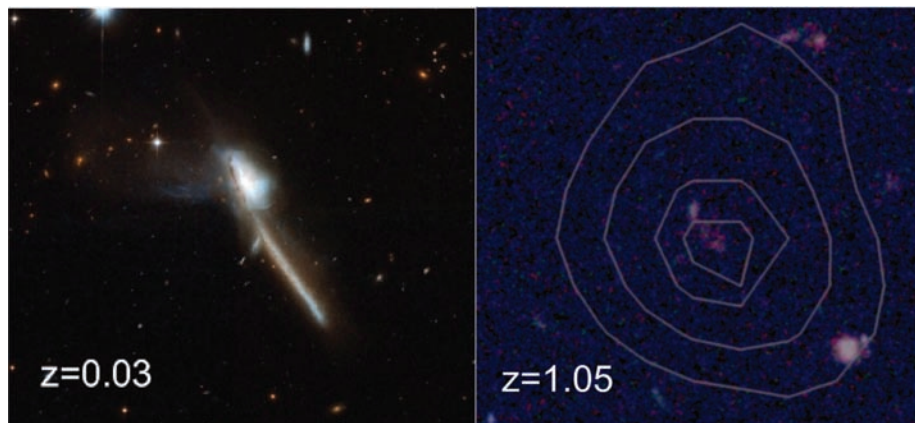


**Fig. 2.** Optical images of two examples of heavily obscured, luminous AGN observed with the Hubble Space Telescope (HST). Filters used are F435W (B) and F814W (I) and V,I,z in the left and right panels, respectively, and the physical size of both images is  $\sim 90 \text{ kpc}$  by  $90 \text{ kpc}$ . Contours in the right panel show the Spitzer emission. (Left) The  $z = 0.03$  prototype ULIRG Mrk 273; (right) a high-redshift heavily obscured quasar candidate in the GOODS-South field, with no x-ray detection. The former is part of the IRAS 1-Jy sample (18) and has clear indications of a major merger, whereas x-ray observations with Suzaku reveal Compton-thick obscuration levels ( $N_{\text{H}} > 10^{24} \text{ cm}^{-2}$ ) and intrinsic quasar-like luminosities (33). The high- $z$  source was selected as a Compton-thick AGN candidate on the basis of its high mid-IR to optical flux ratio and red optical/near-IR colors. [Left panel credit: NASA, European Space Agency (ESA), the Hubble Heritage Team (STScI/AURA)—ESA/Hubble Collaboration, and A. Evans (University of Virginia, Charlottesville, NRAO, Stony Brook University).

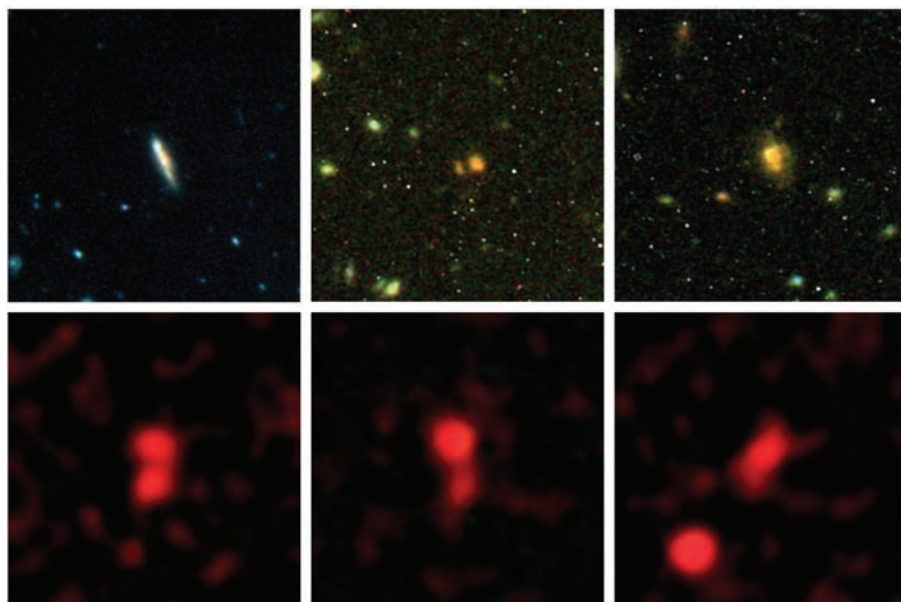


**Fig. 3.** Rest-frame optical images of six mid-IR-selected heavily obscured quasars at  $z \sim 2$  in the Extended Chandra Deep Field-South region. Top images were obtained with the HST-WFC3 (Wide Field Camera 3) camera using the Y, J, and H observations of the Ultra-Deep (left) and GOODS fields. The bottom images were made by combining data in the R, J, and K bands obtained from ground-based telescopes, hence with a spatial resolution about 10 times as large as that of the HST images. All images are  $15 \text{ arc sec}$  by  $15 \text{ arc sec}$ .

2% (8). However, they constitute a significant fraction of the supermassive black hole mass density in the universe (29). Adding the extra obscured accretion reported here, which lasts as long as the optically bright phase, increases our original estimate of the integrated black hole mass density at  $z = 0$  by 4%, to  $4.5 \times 10^5 M_{\odot} \text{Mpc}^{-3}$  (8). Including this additional contribution, the integrated black hole growth in the obscured quasar phase is  $1.3 \times 10^5 M_{\odot} \text{Mpc}^{-3}$ , or  $\sim 30\%$  of the total black hole mass density at  $z = 0$ , in agreement with our conclusion that the obscured quasar phase can harbor a large fraction of the black hole growth (30). Our results are in agreement with recent estimates (26) that suggest an average accretion efficiency of  $\leq 10\%$  even accounting for heavily obscured accretion.

#### References and Notes

1. By quasar, we refer here to the most luminous members of the AGN family, typically  $M_B < -23$ ,  $L_X > 10^{44}$  erg/s or  $L_{\text{bol}} > 10^{45}$  erg/s.
2. M. Schmidt, *Nature* **197**, 1040 (1963).
3. G. T. Richards *et al.*, *Astrophys. J.* **180** (suppl.), 67 (2009).
4. A. J. Barger *et al.*, *Astron. J.* **126**, 632 (2003).
5. N. L. Zakamska *et al.*, *Astron. J.* **126**, 2125 (2003).

6. A. Martínez-Sansigre *et al.*, *Mon. Not. R. Astron. Soc.* **370**, 1479 (2006).
7. R. Gilli, M. Salvati, G. Hasinger, *Astron. Astrophys.* **366**, 407 (2001).
8. E. Treister, C. M. Urry, S. Virani, *Astrophys. J.* **696**, 110 (2009).
9. D. B. Sanders *et al.*, *Astrophys. J.* **325**, 74 (1988).
10. D. B. Sanders, I. F. Mirabel, *Annu. Rev. Astron. Astrophys.* **34**, 749 (1996).
11. J. E. Barnes, L. E. Hernquist, *Astrophys. J.* **370**, L65 (1991).
12. R. Genzel *et al.*, *Astrophys. J.* **498**, 579 (1998).
13. By heavily obscured, we refer here to sources with neutral hydrogen column densities  $N_{\text{H}} > 10^{23} \text{cm}^{-2}$ , enough to hide most of the soft x-rays to optical quasar signatures.
14. P. Tozzi *et al.*, *Astron. Astrophys.* **451**, 457 (2006).
15. D. M. Alexander *et al.*, *Astrophys. J.* **687**, 835 (2008).
16. F. Fiore *et al.*, *Astrophys. J.* **693**, 447 (2009).
17. E. Treister *et al.*, *Astrophys. J.* **706**, 535 (2009).
18. D.-C. Kim, D. B. Sanders, *Astrophys. J.* **119** (suppl.), 41 (1998).
19. P. F. Hopkins, L. Hernquist, T. J. Cox, D. Keres, *Astrophys. J.* **175** (suppl.), 356 (2008).
20. P. F. Hopkins *et al.*, <http://arxiv.org/abs/0906.5357> (2009).
21. D. Marchesini *et al.*, *Astrophys. J.* **701**, 1765 (2009).
22. T. Dahlen *et al.*, *Astrophys. J.* **654**, 172 (2007).
23. G. Hasinger, T. Miyaji, M. Schmidt, *Astron. Astrophys.* **441**, 417 (2005).
24. A. J. Barger *et al.*, *Astron. J.* **129**, 578 (2005).
25. G. T. Richards *et al.*, *Astron. J.* **131**, 2766 (2006).
26. A. Martínez-Sansigre, A. M. Taylor, *Astrophys. J.* **692**, 964 (2009).
27. M. Dietrich, S. Mathur, D. Grupe, S. Komossa, *Astrophys. J.* **696**, 1998 (2009).

28. M. Vestergaard, P. S. Osmer, *Astrophys. J.* **699**, 800 (2009).
29. M. G. Haehnelt, P. Natarajan, M. J. Rees, *Mon. Not. R. Astron. Soc.* **300**, 817 (1998).
30. This integrated value was obtained assuming an accretion efficiency of 0.1 and is in very good agreement with observational results (31), even after incorporating this additional accretion.
31. A. Marconi *et al.*, *Mon. Not. R. Astron. Soc.* **351**, 169 (2004).
32. R. Della Ceca *et al.*, *Astron. Astrophys.* **487**, 119 (2008).
33. S. H. Teng *et al.*, *Astrophys. J.* **691**, 261 (2009).
34. Support for the work of E.T. and K.S. was provided by the National Aeronautics and Space Administration (NASA) through Chandra/Einstein Postdoctoral Fellowship award numbers PF9-90055 and PF9-00069, respectively, issued by the Chandra X-ray Observatory Center, which is operated by the Smithsonian Astrophysical Observatory for and on behalf of NASA under contract NAS8-03060. P.N. acknowledges the Radcliffe Institute for Advanced Study where this work was started. C.M.U. acknowledges support from NSF grant AST-0407295.

#### Supporting Online Material

www.sciencemag.org/cgi/content/full/science.1184246/DC1  
SOM Text  
Figs. S1 and S2  
References

4 November 2009; accepted 17 March 2010

Published online 25 March 2010;

10.1126/science.1184246

Include this information when citing this paper.

# Conversion of Sugars to Lactic Acid Derivatives Using Heterogeneous Zeotype Catalysts

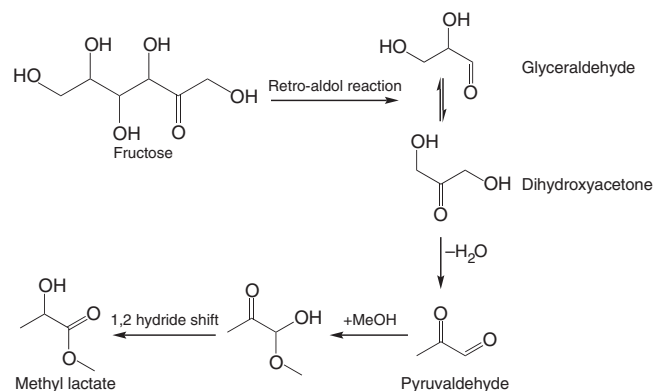
Martin Spangsborg Holm,<sup>1,2,3\*</sup> Shunmugavel Saravanamurugan,<sup>1,2\*</sup> Esben Taarning<sup>2,3†</sup>

Presently, very few compounds of commercial interest are directly accessible from carbohydrates by using nonfermentative approaches. We describe here a catalytic process for the direct formation of methyl lactate from common sugars. Lewis acidic zeotypes, such as Sn-Beta, catalyze the conversion of mono- and disaccharides that are dissolved in methanol to methyl lactate at 160°C. With sucrose as the substrate, methyl lactate yield reaches 68%, and the heterogeneous catalyst can be easily recovered by filtration and reused multiple times after calcination without any substantial change in the product selectivity.

Carbohydrates represent the largest fraction of biomass, and various strategies for their efficient use as a commercial chemical feedstock are being established in the interest of supplementing, and ultimately replacing, petroleum (1–4). The thermal instability of carbohydrates is a major obstacle in this regard, and biochemical processes have proven to be more applicable than catalytic ones, in part because of their ability to operate at low temper-

atures. On the other hand, catalysis often presents improved process design options, resulting in higher productivity and reduced costs related to product work-up. Indeed, catalysis has proven to

**Fig. 1.** Proposed reaction pathway for the conversion of fructose to methyl lactate. The reaction formally comprises a retro aldol fragmentation of fructose and isomerization-esterification of the trioses.



<sup>1</sup>Centre for Catalysis and Sustainable Chemistry, Department of Chemistry, Technical University of Denmark, Anker Engelundsvej 1, 2800 Kongens Lyngby, Denmark. <sup>2</sup>Center for Sustainable and Green Chemistry, Department of Chemistry, Technical University of Denmark, Anker Engelundsvej 1, 2800 Kongens Lyngby, Denmark. <sup>3</sup>Haldor Topsøe A/S, Nymøllevej 55, 2800 Kongens Lyngby, Denmark.

\*These authors contributed equally to this work.

†To whom correspondence should be addressed. E-mail: esta@topsoe.dk